Structures of Photolyzed Carboxymyoglobin†

Frank G. Fiamingo and James O. Alben*
Department of Physiological Chemistry, College of Medicine, The Ohio State University, Columbus, Ohio 43210
Received April 30, 1985; Revised Manuscript Received August 21, 1985

ABSTRACT: The structures of photoactivated carboxymyoglobin (Mb*CO) at temperatures to 10 K have been investigated by Fourier transform infrared (FT-IR) spectroscopy, visible spectroscopy, and near-infrared spectroscopy. Two energy states for *CO are observed by FT-IR, which are altered in frequency by 94% and 88% of the difference from the ground-state heme CO toward free CO gas [Alben, J. O., Beece, D., Bowne, S. F., Doster, W., Eisenstein, L. Frauenfelder, H., Good, D., McDonald, J. D., Marden, M. C., Moh, P. P., Reinisch, L., Reynolds, A. H., Shyamsundar, E., & Yue, K. T. (1982) *Proc. Natl. Acad. Sci. U.S.A. 79*, 3744–3748]. Ground-state MbCO shows no absorption in the near-infrared from 700 to 1200 nm. Conversely, Mb*CO shows an absorption near 766 nm, similar to that of ferrous myoglobin (deoxy-Mb) at 758 nm. These data are compared with Mössbauer isomer shifts and quadrupole splitting [Spartalian, K., Lang, G., & Yonetani, T. (1976) *Biochim. Biophys. Acta 428*, 281–290] and magnetic susceptibility measurements [Roder, H., Berendzen, J., Bowne, S. F., Frauenfelder, H., Sauke, T. B., Shyamsunder, E., & Weissman, M. B. (1984) *Proc. Natl. Acad. Sci. U.S.A. 81*, 2359–2363], which clearly indicate that the iron in both Mb*CO and deoxy-Mb is in the high-spin Fe(II) state, as does the heme transition in the Soret [Iizuka, T., Yamamoto, H., Kotani, M., & Yonetani, T. (1974) *Biochim. Biophys. Acta 371*, 126–139]. Thus the electronic structure of iron in Mb*CO is nearly identical with that of deoxy-Mb, and *CO is only slightly perturbed from the free gas. These data appear to be at odds with a recent interpretation of extended X-ray absorption fine structure data for Mb*CO reported by Chance et al. [Chance, B., Fischetti, R., & Powers, L. (1983) *Biochemistry 22*, 3820–3829] and Powers et al. [Powers, L. Sessler, J. L., Woolery, G. L., & Chance, B. (1984) *Biochemistry 23*, 5519–5523]. Possible reasons for these discrepancies are presented with structural models that are consistent with all spectroscopic data.

Myoglobin is the simplest oxygen carrier among heme proteins, and as such it serves as a model for comparison with more complicated systems. Photolysis of its carbon monoxide complex at low temperatures provides information about fundamental processes such as molecular tunneling and weak interactions that modulate catalytic activities. It is therefore essential, where differences of interpretation arise, to carefully examine their bases and to suggest possible solutions. Recent studies of photolyzed carboxymyoglobin by EXAFS[1] have been interpreted to indicate that the Fe–CO distance is increased by only 0.05 Å relative to that in unphotolyzed MbCO. We here present data from many sources that indicate a different picture.

Infrared difference spectra (Alben et al., 1982) of carboxymyoglobin show the major CO vibrational frequency to be shifted from 1945 cm^{-1} when bound to heme iron to 2131 cm^{-1} after photodissociation at 20 K. This is a shift of 186 cm^{-1}, which is 94% of the frequency difference between carboxymyoglobin and free CO gas (2143 cm^{-1}) or CO in a frozen argon matrix, and implies that the photodissociated CO is at most only weakly influenced by the iron. This conclusion is difficult to reconcile with the short displacement suggested from extended X-ray absorption fine structure. Chance and co-workers have recently reported low-temperature EXAFS data for carboxymyoglobin (Chance et al., 1983a,b, 1982; Fischetti et al., 1981; Powers, 1982) and have interpreted this to require a displacement of the CO upon photolysis of not more than 0.05 Å. Alternative explanations are the possibilities that a significant fraction of CO may never have been photodissociated from the iron in the optically thick solution that was used to measure the EXAFS data or that the treated EXAFS data are too insensitive to detect an alteration in one-sixth of the first-shell atoms surrounding the iron. The authors indicated that the MbCO sample was illuminated until no further structural change could be detected. However, as we have shown (Fiamingo & Alben, 1985) for an optically dense solution, this criterion may not be sufficient to conclude that complete photolysis of the sample has occurred.

These studies lead to an alternative interpretation of the structure of photolyzed carboxymyoglobin (Mb*CO). Experimental infrared data presented here and elsewhere (Alben et al., 1982) and data from this and other laboratories utilizing visible and near-infrared (Iizuka et al., 1974), Mössbauer (Spartalian et al., 1976), magnetic susceptibility (Roder et al., 1984), magnetic circular dichroism (Brittain et al., 1982; Sharonov et al., 1982), and resonance Raman (Argade et al., 1984) spectroscopies all suggest that the structure of Mb*CO consists of a high-spin ferrous heme very similar to, but not identical with, deoxy-Mb and a photodissociated CO that forms only weak attachments with the surrounding heme pocket resulting in only minor perturbations to the heme. Some or all of these perturbations may result from incomplete relaxation of the protein at the low temperatures required for these studies.

Materials and Methods

Sperm whale myoglobin was obtained from Pentex and used without further purification. The myoglobin was dissolved in distilled water, centrifuged for 1 h at 5000 rpm, and concentrated to about 12–16 mM either in an Amicon pressure filter

† This work was supported in part by Grants HL-17839, HL-28144, and RR-01739 from the National Institutes of Health.

[1] Abbreviations: EXAFS, extended X-ray absorption fine structure; MCD, magnetic circular dichroism; IR, infrared; FT-IR, Fourier transform infrared; MbCO, ferrous carboxymyoglobin; Mb*CO, photodissociated ferrous carboxymyoglobin; deoxy-Mb, ferrous myoglobin; TPP, tetraphenylporphyrin; Py, pyridine; THF, tetrahydrofuran; Hb, hemoglobin; deut, deuteroporphyrin; Proto IX, protoporphyrin IX.

0006-2960/85/0424-7964$01.50/0

(for large volumes) or in a Minicon ultrafiltration device (for small volumes), both manufactured by Amicon Corp., Lexington, MA. The protein solutions were then deaerated by repeated evacuation and refilling with argon. Reduction was accomplished by a slight stoichiometric excess of 1 M deoxygenated dithionite solution buffered with 1 M potassium phosphate to pH 7.4 (the pH of the buffer was 8.6 before dithionite addition). The aqueous MbCO sample was then equilibrated with CO after evacuation and inserted between a pair of CaF_2 windows with a 0.095-mm spacer.

The glycerol-extracted MbCO sample was prepared as follows. To a 5-mL aliquot of aqueous MbCO was added 0.5 mL of CO-saturated glycerol. This was then put into a Visking No. 8 dialysis tubing and inserted within a 100-mL test tube filled with CO and CO-saturated glycerol, to extract the water. The resultant protein paste was squeezed onto a CaF_2 window with a 0.38-mm spacer and pressed with a second window before being frozen in a helium refrigerator. Glycerol-extracted carboxyhemoglobin was prepared from aqueous carboxyhemoglobin in a similar manner.

Low temperatures (10–280 K) were conveniently obtained by use of a Lake Shore Cryotronics helium refrigerator, Model LTS-21-D70C. Cryostat cell temperature was measured by use of a Lake Shore Cryotronics digital thermometer, Model DRC-70, with a calibrated silicon diode probe.

Infrared spectra were obtained with a Digilab FTS-14D infrared interferometer fitted with an InSb detector cooled by liquid nitrogen. Interferograms were collected at either 1 or 2 cm^{-1} resolution through a 15-bit A/D converter and a signal-averaged into 32-bit computer words, which were used for all further computations. Single-beam spectra result from the real part of the Fourier transforms of 8192 signal-averaged interferograms. There was no additional averaging or smoothing of the data.

Visible and near-infrared spectra were obtained with a Cary Model 17DX spectrometer adapted to be controlled by a microprocessor with the On-Line Instrument System Model 3820 data system. At each wavelength eight light-chopper cycles were signal-averaged before progressing to the next data point (wavelength), which required about 15 min to collect a scan of 400 data points. The identical sample was observed in both the visible and infrared spectrometers. The sample concentration could be determined from the visible [a = 12.2 mM^{-1} cm^{-1} at 579 nm and room temperature (Antonini & Brunori, 1971)] or mid-infrared [B = 30.4 ± 0.2 mM^{-1} cm^{-2} at 1945 cm^{-1} (Yen, 1971); B = 1.4 ± 0.1 mM^{-1} cm^{-2} at 2131 cm^{-1} (Alben et al., 1982)] spectra.

Photodissociation of heme–CO was accomplished with continuous radiation from a 500-W tungsten lamp focussed through a slide projector and optically filtered through glass and water.

Results

Two separate samples of sperm whale muscle MbCO were observed with both the Fourier transform infrared and the visible–near-infrared spectrometers. In one sample the protein remained dissolved in water, and in the second the water was extracted with glycerol, as detailed under Materials and Methods. The aqueous sample had a measured absorbance of 1.62 at 579 nm, and the glycerol sample had an estimated absorbance of 24 ± 5 at 579 nm. The aqueous sample was easily photolyzed, and quantitative data refer to this sample. The glycerol-extracted sample could not be completely photolyzed even after exposure to a 500-W projector lamp for 11 h, even though bright red light was transmitted through the thick myoglobin sample (Fiamingo & Alben, 1985). The

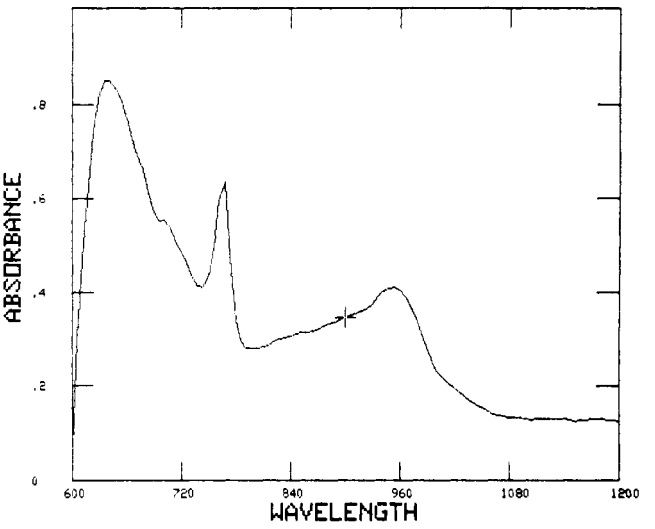

FIGURE 1: Mb*CO–MbCO near-infrared absorbance difference observed with a glycerol-extracted sample after several cycles of photolysis and relaxation. This spectrum was measured at 14 K after relaxation (overnight) at 180 K. The conformation indicator band of Iizuka et al. (1974) appears at 766 ● 1 nm with a half-width of 18 nm in this optically thick sample. The broad band at 953 nm is also due to the photolyzed species. The peak at 640 nm reflects a frequency difference in the α-band of the two forms.

degree of FeCO photolysis could be readily ascertained by observation of the 1945-cm^{-1} mid-infrared transmission band before and after photolysis (Alben et al., 1982; Fiamingo & Alben, 1985) or, in the case of such a highly absorbing sample as this, from the FeCO band at 1901 cm^{-1} arising from the 1.31% natural abundance of the heavy isotopes $^{13}C^{16}O$ and $^{12}C^{18}O$ (Fiamingo & Alben, 1985). The before and after photolysis near-infrared absorbance difference spectrum of this optically dense glycerol sample is shown in Figure 1. For both samples a Mb*CO "conformation" band similar to that reported by Iizuka et al. (1974) at 772 nm was observed at 766 ± 1 nm along with a second broader band at 953 nm. The former band is only slightly shifted from the deoxy-Mb band at 757.6 nm that has been assigned to an iron $b_{1g}(d_{x^2-y^2}) \rightarrow$ porphyrin $e_g(\pi^*)$ charge-transfer transition by Makinen & Churg (1983) in deoxy-Mb and to a porphyrin $a_{2u}(\pi) \rightarrow$ iron d_{yz} charge-transfer transition by Eaton et al. (1978) in deoxy-Hb. A 930-nm band from deoxy-Mb has been assigned to an iron $d_{xz} \rightarrow$ porphyrin $e_g(\pi^*)$ charge-transfer transition (Makinen & Churg, 1983).

The concentration estimates of the aqueous sample from the 579-nm peak height at room temperature [a = 12.2 mM^{-1} cm^{-1} (Antonini & Brunoni, 1971)], and from the integrated intensity of the FeCO vibrational absorbance envelope at low temperature [B = 30.4 ± 0.2 mM^{-1} cm^{-2} at room temperature (Yen, 1971)], were the same within experimental error at 14 ± 1 mM. The absorbance enhancement factor, the ratio of the absorbance of the frozen sample at low temperature with the solution absorbance at room temperature (Vincent et al., 1982), must then be either unity or some nonunity value that is the same at both wavelengths. Since there is a 9-fold difference in wavelength between 579 nm (17 271 cm^{-1}) and 1945 cm^{-1} (5140 nm), even a very weak wavelength dependence from light scattering would be observable. The absorptivity of the near-infrared band at 766 nm is then about 0.4 mM^{-1} cm^{-1} measured at 12 K but extrapolated to liquid conditions by the visible and infrared band absorption.

For the optically thick protein sample in glycerol the concentration of the photolyzed species at 2131 cm^{-1} [the B_1 band of Alben et al. (1982)] could be estimated from its integrated

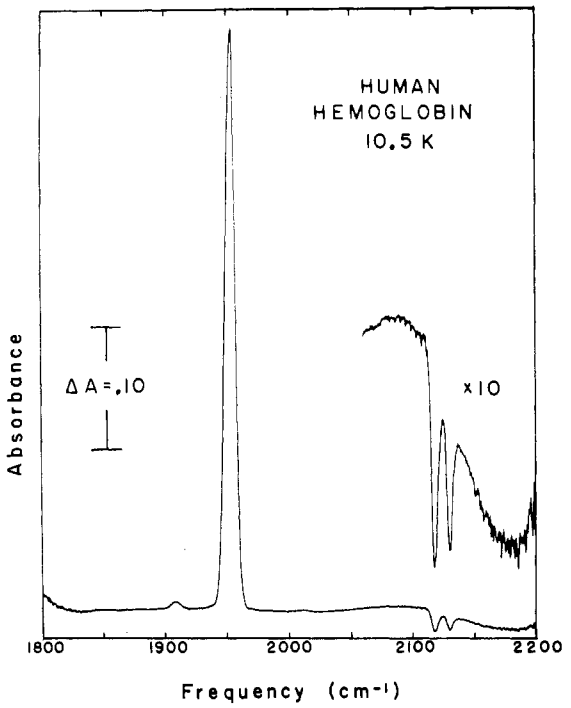

FIGURE 2: FT-IR absorbance difference spectrum of HbCO (in glycerol) before and after photolysis at 10.5 K. The photolyzed CO absorbs at 2131 cm^{-1} (B_1 band) and at 2118 cm^{-1} (B_2 band). The original spectra were collected at 1-cm^{-1} resolution through a sample path length of 0.02 cm.

intensity [$B = 1.4 \pm 0.1$ mM^{-1} cm^{-2} (Alben et al., 1982)]. The original MbCO concentration could then be estimated to be 53 ± 10 mM so that the absorbance at 579 nm was calculated to be 24 ± 5.

In one photolysis experiment we obtained 76 ± 8% photodissociation after 11 h of illumination. Following relaxation at 180 K for 30 min the sample was again illuminated for 11 h, resulting in 39 ± 5% photodissociation (Fiamingo & Alben, 1985). Several more cycles through temperature, including one overnight relaxation at 180 K to assure complete relaxation of Mb*CO, succeeded in making the glycerol-dehydrated sample nearly opaque to mid-infrared light. This probably represented increased light scattering due to the formation of microcrystals during devitrification of the solvent. Such phenomena have been described previously (Vincent et al., 1982; Estabrook, 1956; Keilin & Hartree, 1950).

A spectrum of the optically dense sample before photolysis showed a small amount of deoxy-Mb at 758 nm, the same frequency as that observed by Iizuka et al. (1974) for deoxy-Mb. The presence in this sample of a small fraction of deoxymyoglobin is not unreasonable with its history of several cycles of photolysis and relaxation under vacuum during collection of the mid-infrared data. The state of iron-coordinated or photodissociated CO in carboxymyoglobin is very well-defined by its vibrational absorption in the infrared. The Fe–CO absorptions have been designated as A states (A_0, A_1, and A_2), while the photodissociated forms are called B states (B_0, B_1, and B_2), from studies with myoglobin from sperm whale muscle. While the B_2 band is large in samples at 4–10 K (Alben et al., 1982), it was nearly absent throughout the observation range of this sample, 12–15 K. The B_1 and B_2 absorption bands of photolyzed CO are also clearly observed in myocytes from rat heart (Alben et al., unpublished results), and in human hemoglobin (Figure 2). They are thus independent of the multiplicity of A states [(FeCO)heme] such as those that are prominently observed in myoglobin from sperm whale and beef heart (Alben et al., 1982; Makinen et al., 1979) and represent two distinct local environments of photolyzed CO within the frozen pocket.

The B_2 absorption in Hb*CO is more prominant at 10 K than the corresponding absorption in Mb*CO. This has been observed with Hb*CO in frozen aqueous solution and in glycerol-dehydrated preparations and may be due to the more constrained heme pocket in hemoglobin. The difference between the B_1 and B_2 bands in Hb*CO is not due to a difference between the α and β chains as evidenced by the fact that at 40 K only the B_1 band is observed, while at 10 K the B_2 band is more intense then the B_1 band. We observed only one $Fe^{12}C^{16}O$ band (A_1; 1953 cm^{-1} in glycerol at 10 K) that consists of overlapping absorptions from the α and β chains in this HbCO sample. An A_0 band is sometimes observed near 1968 cm^{-1}. HbCO does not exhibit an A_2 band as observed in MbCO.

Discussion

The interpretation of the EXAFS data of Chance and coworkers (Chance et al., 1983a,b, 1982; Fischetti et al., 1981; Powers, 1982; Powers et al., 1984) is based in part upon the observation of negligible change in the population of the photolyzed species after repeated light flashes. As we have shown, this condition should not by itself be construed as proof of complete photolysis (Fiamingo & Alben, 1985). Nor should the observation of the loss of the MbCO visible reflectance spectrum be so construed, since this observation might also be produced by a small amount of light reflected to the back surface rather than transmitted through the sample. When the 7150–7200-eV region of the X-ray absorption spectrum (Chance et al., 1983a) is used as an indicator of structural change, the photolyzed sample after "saturation" with repetitive flashes produces a change relative to the unphotolyzed sample that is 60% of that of deoxy-Mb. Chance and coworkers have attributed the small change observed in the EXAFS spectrum after illumination to a displacement of the CO upon photolysis by less than 0.05 Å. This conclusion appears to be inconsistent with the results from other techniques, several of which are presented in Table I and discussed as follows.

Mössbauer spectra reflect the energy-level shifts of the iron nucleus. The isomer shift and quadrupole splitting of Spartalian et al. (1976), listed in Table I, show that Mb*CO is very similar to deoxy-Mb, being 96 and 104%, respectively, of the difference between MbCO and deoxy-Mb for these two measurements at 4.2 K. The data clearly indicate a high-spin ($S = 2$) state for the iron in Mb*CO with only minor differences between this form and deoxy-Mb.

The mid-infrared spectra of Alben et al. (1982) (Figures 2–4 of that work) show absorptions at the vibrational stretching frequency of the CO. Interactions between the CO and its surroundings perturb its dipole moment and shift its frequency relative to that of the free gas (centered at 2143 cm^{-1}). When the CO is bound to the iron, the major $^{12}C^{16}O$ band (A_1) appears at 1945 cm^{-1}, and upon photodissociation it appears at 2131 (B_1) and 2119 (B_2) cm^{-1}. The B_2 band was observed only below 20 K. These photolyzed states represent changes of 94 and 88%, respectively, toward the frequency of the free gas. This indicates that the photolyzed CO is only weakly influenced by adjacent dipoles.

The Soret and near-infrared transitions reflect the electronic transitions of the heme. The spectra of Iizuka et al. (1974) show Mb*CO to be much more similar to deoxy-Mb than to MbCO. The low-temperature Soret spectra show MbCO at 424 nm and the photodissociated species at 437 nm. At room

Table I: Myoglobin Experimental Parameters[a]

sample	Mössbauer[b] iron isomer shift (mm/s)	Mössbauer[b] iron quadrupole splitting ΔE (mm/s)	mid-infrared,[c] carbonyl stretching frequency (cm^{-1}) $^{12}C^{16}O$	mid-infrared,[c] carbonyl stretching frequency (cm^{-1}) $^{13}C^{16}O$	near-infrared,[d,e,f] heme electronic transitions (nm) absorbance	near-infrared,[d,e,f] heme electronic transitions (nm) MCD[f]	Soret,[e] heme electronic transitions (nm)	magnetic susceptibility,[g] heme electronic structures: tetragonal crystal field parameter D (cm^{-1})	magnetic susceptibility,[g] heme electronic structures: rhombic crystal field parameter E (cm^{-1})
MbCO	0.368	0.27	1945	1901	not obsd	not obsd	424	diamagnetic	diamagnetic
Mb*CO	0.88	2.28	2119	2073	772,[e] 766[d]	766	437	5.0 ± 0.5	0.8 ± 0.3
			2131	2084					
deoxy-Mb	0.911	2.20			758[d,e]	757	434	5.7 ± 0.3	0 ± 0.3
CO			2143	2096					

[a] These parameters were obtained from several different techniques used to observe the ligated and photodissociated carboxymyoglobin and compared with those from deoxymyoglobin and free CO gas. [b] Data from Spartalian et al. (1976). The values were obtained by using Lorentzian band shapes and in some cases represent a weighted average of two similar bands. [c] Data from this work and Alben et al. (1982). [d] Data from this work. [e] Data from Iizuka et al. (1974). [f] Data from Sharonov et al. (1982). [g] Data from Roder et al. (1984).

temperature deoxy-Mb peaks at 434 nm. The near-infrared spectra show an even greater similarity between deoxy-Mb and Mb*CO, with peaks reported at 758 and 772 nm, respectively, at 4.2 K (we observed 758 and 766 nm at 12–15 K) while *no absorption* was observed for MbCO in this spectral region.

Magnetic circular dichroism measurements by Brittain et al. (1982) and Sharonov et al. (1982) show similar spectra for deoxy-Mb and Mb*CO, indicating that both are high spin ($S = 2$). The Soret band (Brittain et al., 1982) shows a slightly broader and more intense absorbance difference for Mb*CO, where the peak–trough frequency difference is 15 nm for deoxy-Mb and 17 nm for Mb*CO, possibly indicating a change in band shape due to the influence of the photolyzed CO on the porphyrin. The change in the differential molar extinction coefficient at 1.5 K from 27×10^3 to 36×10^3 cm^{-1} M^{-1}, an increase of 33% for Mb*CO over deoxy-Mb, is a less reliable indicator of structural change. It critically depends on knowledge of the concentration, the absorbance enhancement factor (Vincent et al., 1982) for both left and right circularly polarized light, and the depolarization of the light as it travels through each sample (Brittain et al., 1982). The latter two will both be influenced by the form in which the frozen sample solution exists (and thus the amount of light scattering) at the measuring temperature (Vincent et al., 1982; Estabrook, 1956; Keilin & Hartree, 1950). MCD measurements in the near-infrared (Sharonov et al., 1982) show deoxy-Mb at 757 nm and Mb*CO at 766 nm (at 15 K), while MbCO has no MCD absorptions. Argade et al., (1984) have studied the photodissociation of MbCO by resonance Raman spectroscopy. They have concluded that any possible association of the photolyzed *CO with the heme must be such as to have no significant influence on the molecular or electronic structure of the heme. The heme in Mb*CO is thus similar to but not identical with that in deoxymyoglobin.

*Structures of MbCO and Mb*CO.* Neutron diffraction analysis of single crystals of MbCO (Norvell et al., 1975) places the Fe-bound CO molecule at 24° to the heme normal, mostly toward the direction of the nitrogen on pyrrole II. The iron is low spin ($S = 0$) and may be displaced slightly toward the proximal histidine (Norvell et al., 1975). Figure 3a shows the neutron diffraction density of the heme and its surroundings [redrawn from Norvell et al. (1975)], and Figure 3b shows the van der Waals surface, as determined by neutron diffraction, of all atoms within 4 Å of the top surface (CO side) of the heme [redrawn from Hanson & Schoenborn (1981)]. In part b of this figure the bound CO occupies the space between the X (iron position) and Leu B13. These figures suggest that there may be considerable space available within which a photolyzed *CO could oscillate before losing its translational energy by collisions. The oxygen atom of the

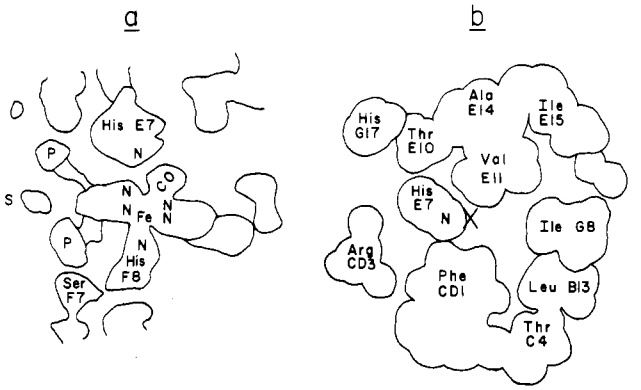

FIGURE 3: MbCO heme environment. Panel a shows the neutron diffraction density of the heme and its surroundings; P designates the propionic acid side chains of the heme and S is a solvent molecule (D_2O). Panel b shows the van der Waals surface, as determined by neutron diffraction, of all atoms within 4 Å of the heme. The view is from the top surface (CO side, opposite the proximal histidine) of the heme. The X marks the iron position. The CO occupies the space between the iron and Leu B13. Panel a was adapted from Figure 2 of Norvell et al. (1975) and panel b from Figure 10a of Hanson & Schoenborn (1981).

CO appeared to have considerable disorder, which prevented quantitation of the Fe–C–O bond angle.

Indeed, three different infrared frequencies (A states) are observed for $Mb^{12}C^{16}O$ (Alben et al., 1982; Makinen et al., 1979), which may indicate three different geometries for the FeCO bond with respect to the heme nitrogens, possibly due to interactions with nearby amino acid residues (Makinen et al., 1979). At low temperature these bands are observed at 1969, 1945, and 1927 cm^{-1} and are designated A_0, A_1, and A_2, respectively (Alben et al., 1982). Theoretical quantum mechanical studies have implied that the bending of the CO bond away from the heme normal greatly facilitates photodissociation by lowering the energy of the excited states (Waleh & Loew, 1982). Upon photolysis following absorption of visible light by the heme, the CO infrared absorption shifts to 2131 cm^{-1} (state B_1), only 12 cm^{-1} below the frequency of the free gas at 2143 cm^{-1}, at which a small fraction of the photolyzed CO is sometimes observed [state B_0; see Alben et al. (1982)]. Below 20 K a third band (Alben et al., 1982) is observed at twice this displacement from the free gas value (state B_2 at 2119 cm^{-1}). A similar pair of bands (B_1 at 2131 cm^{-1} and B_2 at 2118 cm^{-1}) is observed with Hb*CO (Figure 2) at both 10.5 and 21 K, even though the frequencies and distribution of A states (FeCO) are very different between sperm whale MbCO (A_1 at 1945 cm^{-1} and A_2 at 1927 cm^{-1} at 10 K) and human HbCO (A_1 at 1953 cm^{-1} at 10 K; no A_2 state is observed). The B states therefore appear to be common

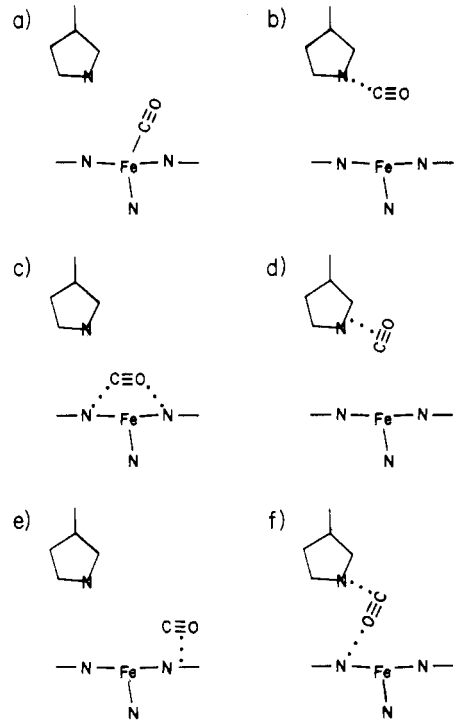

FIGURE 4: Possible CO configurations. (a) FeCO before photolysis. Panels b–f show some possible structures of the photolyzed CO. (b) Dipole–dipole interaction of the CO with the N_ϵ of the distal histidine. (c) Dipole–dipole interaction between CO and the porphyrin. (d) Association of the CO with the distal histidine at other than the N_ϵ. (e) π–π interaction between the CO and the porphyrin. (f) Dipole–dipole interaction of the CO with both the distal histidine and the porphyrin. This illustration represents only a few of the possible modes of interaction.

to photolyzed heme proteins and independent of A-state conformations. These small changes in the infrared vibrational frequency of *CO from that of the noninteracting (free gas) molecule indicate only weak associations of the CO with the heme environment, probably through dipole–dipole or $\pi \rightarrow \pi^*$ interactions. The low-temperature stabilization of the B_2 state and the fact that it has twice the frequency displacement from the free gas value as does the B_1 state suggest that it might be caused by two such weak interactions. This would be consistent with the fact that the greater perturbation (B_2) is observed only at the lower temperatures and that the sum of the areas for B_1 plus B_2 appears to be invariant with temperature, such that only the relative amounts of each change (Alben et al., 1982). Some of the many possible configurations of the B states are illustrated in Figure 4. These few examples fall far short of exhausting all the possible modes of interaction.

Case & Karplus (1979) have helped to narrow the list of accessible possibilities with their theoretical treatment of the dynamics of CO binding and photolysis in myoglobin. The ligand is assumed to be within a rigid protein and is approximated as a neutral sphere. Photolysis consists of removing the Fe–CO bond and giving the ligand an initial kinetic energy. The direction of initial motion was randomly distributed on the distal side of the heme, and the calculation was stopped after 3.75 ps of motion. All interactions were assumed to be energy-conserving, hard-sphere, elastic collisions. Of the 150 trajectories followed, 50 resulted in the CO being trapped in the heme pocket within about 7 Å of its initial position. For 45 trajectories the CO was trapped within the heme pocket but not near the iron. The remaining trajectories resulted in escape of the CO from the protein into the surrounding solvent. Relaxation of our frozen solutions at 120–200 K quickly allowed quantitative recombination of the CO with the iron, so escape routes are not available in the frozen protein. In the model of Case and Karplus most of the *CO was trapped close to the heme between His E7, Val E11, Leu B13, Ile G8, and Phe CD1, some above this space farther from the heme and some above pyrrole I, the space bounded by Val E11, Ala E14, Ile E15, and Ile G8 shown in Figure 3b. When electronic interactions are allowed between the *CO and the protein, the possible stable sites for the *CO may be modified. These sites are stabilized at low temperatures and are identified by the infrared absorptions of *CO.

At the low temperatures employed in the actual experiments not all of those configurations that require movement of certain amino acid residues may be accessible. X-ray diffraction of MbCO shows that the residues about the heme have much less flexibility at 80 K than at 300 K (Hartman et al., 1982). This decrease in flexibility of the protein may explain the observed spectral differences between Mb*CO and deoxy-Mb.

In at least one other heme protein it is known that the photodissociated CO can leave the immediate vicinity of the iron. CO photolyzed from cytochrome *c* oxidase–CO associates with a copper ion that is estimated to lie about 4–6 Å from the iron (Fiamingo et al., 1982). Photolysis causes the quantitative transfer of CO from a cytochrome a_3–Fe complex to Cu_B even at temperatures as low as 10 K. The photolyzed CO must, therefore, have sufficient energy to escape from the Fe complex. Dissociation of Cu_BCO above 140 K results in the quantitative reformation of a_3–FeCO.

In MbCO the iron has zero electron spin, is at most 0.1 Å below the mean nitrogen plane toward the proximal histidine (Norvell et al., 1975), and exhibits a slightly disturbed tetragonal structure. In deoxy-Mb the iron is high spin and 0.42 Å from the plane of the heme nitrogens (Takano, 1977a) and exhibits a pentacoordinate square-pyramidal structure. While Mössbauer (Spartalian et al., 1976), magnetic susceptibility (Roder et al., 1984), and MCD (Brittain et al., 1982; Sharonov et al., 1982) measurements show the iron of Mb* to be high spin, it may not be possible for it to completely assume the deoxy geometry due to incomplete relaxation of the protein at low temperature. Alternatively, the presence of the *CO within the pocket, rather than protein rigidity, may cause these small differences. The *CO interaction with the protein is, however, quite weak and can be expected to cause no more than a minor perturbation of the heme geometry.

It is also instructive to compare iron–ligand distances among several types of heme complexes. A value of 1.7–1.8 Å is reported for Fe(II)–CO complexes in Fe(TPP)(Py)CO (Peng & Ibers, 1976), Fe(TPP)(SC_2H_5)CO (Caron et al., 1979), and Fe(deut)(THF)CO (Scheidt et al., 1981). A similar iron–carbon distance has been reported for the low-spin Fe(III) complex, Fe(TPP)(Py)CN (1.908 Å; Scheidt & Gutermann, 1983). High-spin Fe(III) halide complexes yield iron–ligand distances [Fe^{III}(Proto IX)Cl, 2.218 Å (Koenig, 1965); Fe^{III}(TPP)F, 1.792 Å (Anzai et al., 1981)] that are 0–0.4 Å greater than those reported for low-spin complexes.

In Mb*CO the CO is only slightly perturbed from the free gas, and so at most could only be associated with Fe(II) by weak dipole interactions, rather than by the charge interactions of ionic Fe(III) complexes, which are especially strong in the fluoride derivative. A corresponding increase in Fe*CO distance over ionic $Fe(III)^+$–L^- distance is expected. It may be noted that a water molecule has been reported in the heme pocket of deoxyerthrocruorin at 3.1 Å from the Fe (Steigemann et al., 1979). Fermi (1975) reported the presence of a water molecule in the α-heme pocket of deoxyhemoglobin that

was in van der Waals contact with Fe (at 3.6 Å), N of pyrrole II (at 2.9 Å), and C_{γ_2} of Val E11 and hydrogen-bonded with N_ϵ (at 3.0 Å) of His E7. Takano (1977b) has reported a water molecule within the heme pocket of deoxymyoglobin that is not in contact with the Fe. It was hydrogen-bonded to His E7 (at 3.2 Å) and in contact with the porphyrin, being 3.0 Å from C_1 of pyrrole II. There appears to be ample space for CO to be within the heme pocket and not in contact with the iron. An increase in the Fe–C distance with photolysis of MbCO of 0.05 Å, as suggested by Chance and Powers (Chance et al., 1983a; Powers et al, 1984), would require the CO to remain within the first coordination shell of iron. This appears to be inconsistent with all other spectroscopic data.

Concerns of EXAFS Data Analysis. The preceding analysis leads us to question the uniqueness of the interpretation that has been given to the EXAFS measurements of Mb*CO (Powers et al., 1984; Chance et al., 1983a; Powers, 1982), and to reexamine some of the assumptions that are used for data analysis. It is especially disturbing that EXAFS measurements of myoglobin from sperm whale have not distinguished multiple heme–CO conformers (A states), since X-ray frequencies are very fast compared to translational or rotational molecular motions, as are also infrared CO vibrations. At room temperature these motions are fast relative to ^{13}CO NMR frequencies, where a single band was observed with MbCO from beef heart by Caughey et al. (1981). We have also observed a single ^{13}CO NMR absorption at 75.43 MHz with MbCO from sperm whale at 207.5 ppm that is well described by a symmetrical Lorentzian function with full-width at half-maximum (fwhm) = 0.415 ppm at 24 °C. It may be that the infrared A states represent rotational conformers around the Fe–C bond with little difference in iron first-shell bond distances, in which case EXAFS measurements are expected to be insensitive since only radial distances can normally be extracted. However, it is interesting to note that Powers et al. (1984) now claim that heme–CO complexes in which the CO is variously bent from the heme perpendicular can be distinguished with EXAFS by comparison with model compounds with known structure. If so, it is not clear why multiple A states, which are especially prominent in MbCO from sperm whale, are not observed by these authors.

The theoretical basis for extended X-ray absorption fine structure (EXAFS) and its analysis have been described in detail elsewhere (Powers, 1982; Cramer et al., 1978a,b; Cramer & Hodgson, 1979; Brown & Doniach, 1980; Brown, 1980; Lytle et al., 1980; Doniach et al., 1980; Peisach et al., 1982; Eisenberger et al., 1978; Philips et al., 1982; Woolery et al., 1984). Many of the assumptions that are inherent in data analysis have been described by Cramer & Hodgson (1979), Powers (1982), and Brown (1980). Briefly, the method used by Powers and Chance (Powers, 1982; Chance et al., 1983a; Woolery et al., 1984) is as follows. First the EXAFS portion of the data is extracted by subtraction of an extrapolated base line, subtraction of near-edge components, and fitting of cubic splines to remove residual base-line components. Next the residual oscillatory component (EXAFS) is converted to k space, multiplied by k^3, and Fourier-filtered to remove effects of higher order scattering. The residual inverse Fourier transform is then compared with similarly obtained data from model compounds, or with appropriate mathematical models. This procedure of multiplication of the k-space spectrum by k^3 followed by Fourier filtering may be justified for simple compounds that are described by only a single first-shell radial distance from a heavy central atom, but it introduces mathematical artifacts due to the finite length of the data set (Brown, 1980) and in addition filters the random (noise) components that are needed to distinguish errors of measurement from errors in the applied model. This suggests that it might be safer to compare the appropriate model with observed EXAFS data before the Fourier filter as reported by Cramer et al. (1978a) and Phillips et al. (1982). Phase corrections would then be directly part of the fitting procedure. EXAFS measurements that are better able to distinguish not only first-shell pyrrole nitrogen atoms but also α- and γ-carbon atoms of the heme have been reported (Hahn et al., 1982; Cramer et al., 1978b). Similar measurements appear to be needed for derivatives of myoglobin in order to resolve the apparent discrepancies in interpretation of these spectral data.

Considering all the uncertainties discussed above, it would appear unlikely that the position of the photolyzed CO could be discerned with confidence by EXAFS under the experimental conditions for data collection and analysis that were reported by Chance and Powers. This may explain the failure to observe structures that correspond to the B_1 and B_2 states of photolyzed Mb*CO. It has been suggested (B. Chance, personal communication) that a model for Mb*CO in which *CO is bound at the iron parallel to the heme plane might satisfy both the high-infrared frequency and the model proposed by Chance and Powers (Chance et al., 1983a; Powers et al., 1984; Powers, 1982) in which the photolyzed CO differs from that in unphotolyzed MbCO by only 0.05 Å. Such an explanation would require that 6- and 7-coordinate heme–CO species could not be distinguished by present EXAFS data. It appears equally likely that 5- and 6-coordinate species are also not distinguished by these data.

Conclusions

All of the experimental data appear to agree with the following model for MbCO photolyzed at low temperatures. The high-spin iron and porphyrin are nearly identical with those in deoxy-Mb, the differences being due to restricted relaxation of the protein, which also restricts movement of the porphyrin away from the proximal (F8) histidine. Photolysis provides sufficient kinetic energy to the CO that it bounces among many locations within the frozen hemoprotein pocket until stabilized by one or two weak dipole interactions. The photolyzed CO is not observed by EXAFS because of increased steric disorder coupled with an increased radial distance from the iron. The present EXAFS data do not appear to be able to distinguish the number of atoms within the first shell nor among mixtures of partially photolyzed MbCO.

The purpose of this paper is not to criticize the experimental efforts of Chance and Powers, for indeed their efforts have been monumental. Rather the discrepancies we find between interpretations of EXAFS data of Chance and Powers and interpretations of spectroscopic data from many laboratories demands a reexamination of the basis for these interpretations. Our conclusions are that the present EXAFS data of Mb*CO may not be sufficient to distinguish unique first-shell distances that contain more than one Fe–X distance, nor to distinguish between five, six, or seven first-shell atoms.

The wider concern is that questions we have raised with regard to interpretation of EXAFS data for MbCO and its photoproduct become much more severe with larger biomolecules. We suggest that successful application of EXAFS to structural studies of biological macromolecules will require much improved signal/noise, much higher resolution, and freedom from computational artifacts such as those introduced by k^3 multiplication of $\chi(k)$ before Fourier transformation of a finite data array.

ACKNOWLEDGMENTS

We thank S. Bowne, B. Chance, S. Cramer, L. Eisenstein, H. Frauenfelder, D. Good, L. Powers, A. Reynolds, D. Rousseau, and R. Scott for illuminating discussions and B. Chance and H. Frauenfelder for providing copies of their manuscripts in advance of publication. We especially thank B. Chance and L. Powers for detailed discussions of photolysis, EXAFS, and the difficulties that attend these experimental approaches.

Registry No. CO, 630-08-0; Fe, 7439-89-6.

REFERENCES

Alben, J. O., Beece, D., Bowne, S. F., Doster, W., Eisenstein, L., Frauenfelder, H., Good, McDonald, J. D., Marden, M. C., Moh, P. P., Reinisch, L., Reynolds, A. H., Shyamsundar, E., & Yue, K. T. (1982) *Proc. Natl. Acad. Sci. U.S.A. 79*, 3744–3748.

Antonini, E., & Brunori, M. (1971) *Hemoglobin and Myoglobin in their Reactions with Ligands*, p 19, American Elsevier, New York.

Anzai, K., Hatano, K., Lee, Y. J., & Scheidt, W. R. (1981) *Inorg. Chem. 20*, 2337–2339.

Argade, P. V., Scott, T. W., Friedman, J. M., & Rousseau, D. L. (1984) *Biophys. J. 45*, 366a.

Brittain, T., Greenwood, C., Springall, J. P., & Thomson, A. J. (1982) *Biochim. Biophys. Acta 703*, 117–128.

Brown, G. S. (1980) in *Synchrotron Radiation Research* (Winick, H., & Doniach, S., Eds.) Chapter 11, pp 387–400, Plenum Press, New York.

Brown, G. S., & Doniach, S. (1980) in *Synchrotron Radiation Research* (Winick, H. & Doniach, S., Eds.) Chapter 10, pp 353–386, Plenum Press, New York.

Caron, C., Mitschler, A., Riviere, G., Ricardi, L., Schappacher, M., & Weiss, R. (1979) *J. Am. Chem. Soc. 101*, 7401–7402.

Case, D. A., & Karplus, M. (1979) *J. Mol. Biol. 132*, 343–368.

Caughey, W. S., Shimada, H., Choc, M. G., & Tucker, M. P. (1981) *Proc. Natl. Acad. Sci. U.S.A. 78*, 2903–2907.

Chance, B., Fischetti, R., Sivaram, A., & Powers, L. (1982) *Biophys. J. 37*, 368a.

Chance, B., Fischetti, R., & Powers, L. (1983a) *Biochemistry 22*, 3820–3829.

Chance, B., Korzun R., Fischetti, R., & Powers, L. (1983b) *Biophys. J. 41*, 416a.

Cramer, S. P., & Hodgson, K. O. (1979) *Prog. Inorg. Chem. 25*, 2–39.

Cramer, S. P., Hodgson, K. O., Stiefel, E. I., & Newton, W. E. (1978a) *J. Am. Chem. Soc. 100*, 2748–2761.

Cramer, S. P., Dawson, J. W., Hodgson, K. O., & Hager, L. P. (1978b) *J. Am. Chem. Soc. 100*, 7282–7290.

Doniach, S., Eisenberger, P., & Hodgson, K. O. (1980) in *Synchrotron Radiation Research* (Winick, H., & Doniach, S., Eds.) Chapter 13, pp 425–458, Plenum Press, New York.

Eaton, W. A., Hanson, L. K., Stephens, P. J., Sutherland, J. C., & Dunn, J. B. R. (1978) *J. Am. Chem. Soc. 100*, 4991–5003.

Eisenberger, P., Shulman, R. G., Kincaid, B. M., Brown, G. S., & Ogawa, S. (1978) *Nature (London) 274*, 30–34.

Estabrook, R. W. (1956) *J. Biol. Chem. 223*, 781–794.

Fermi, G. (1975) *J. Mol. Biol. 97*, 237–256.

Fiamingo, F. G., & Alben, J. O. (1985) *Appl. Spectrosc. 39*, 116–123.

Fiamingo, F. G., Altschuld, R. A., Moh, P. P., & Alben, J. O. (1982) *J. Biol. Chem. 257*, 1639–1650.

Fischetti, R., Sivaram, A., & Chance, B. (1981) Abstracts of the VIIth International Biophysics Congress and the IIIrd Pan-American Biochemistry Congress, Mexico City, Aug 1981, p 322.

Hahn, J. E., Hodgson, K. O., Andersson, L. A., & Dawson, J. H. (1982) *J. Biol. Chem. 257*, 10924–10941.

Hanson, J. C., & Schoenborn, B. P. (1981) *J. Mol. Biol. 153*, 117–146.

Hartmann, H., Parak, F., Steigemann, W., Petsko, G. A., Ringe Ponzi, D., & Frauenfelder, H. (1982) *Proc. Natl. Acad. Sci. U.S.A. 79*, 4967–4971.

Hoard, J. L., Cohen, G. H., & Glick, M. D. (1967) *J. Am. Chem. Soc. 89*, 1992–1996.

Iizuka, T., Yamamoto, H., Kotani, M., & Yonetani, T. (1974) *Biochim. Biophys. Acta 371*, 126–139.

Keilin, D., & Hartree, E. F. (1950) *Nature (London) 165*, 504–505.

Koenig, D. F. (1965) *Acta Crystallogr. 18*, 663–673.

Lytle, F. W., Via, G. H., & Sinfelt, J. H. (1980) in *Synchrotron Radiation Research* (Winick, H., & Doniach, S., Eds.) Chapter 12, pp 401–424, Plenum Press, New York.

Makinen, M. W., & Churg, A. K. (1983) in *Iron Porphyrins* (Lever, A. B. P., & Gray, H. B., Eds.) Part I, Chapter 3, pp 191–192, Addison-Wesley, Reading, MA.

Makinen, M. W., Houtchens, R. A., & Caughey, W. S. (1979) *Proc. Natl. Acad. Sci. U.S.A. 76*, 6042–6046.

Norvell, J. C., Nunes, A. C., & Schoenborn, B. P. (1975) *Science (Washington, D.C.) 190*, 568–570.

Peisach, J., Powers, L. Blumberg, W. E., & Chance, B. (1982) *Biophys. J. 38*, 277–285.

Peng, S.-M., & Ibers, J. A. (1976) *J. Am. Chem. Soc. 98*, 8032–8036.

Philips, J. C., Bordos, J., Foote, A. M., Koch, M. H. J., & Moody, M. F. (1982) *Biochemistry 21*, 830–834.

Powers, L. (1982) *Biochim. Biophys. Acta 683*, 1–38.

Powers, L., Sessler, J. L., Woolery, G. L., & Chance, B. (1984) *Biochemistry 23*, 5519–5523.

Roder, H., Berendzen, J., Bowne, S. F., Frauenfelder, H., Sauke, T. B., Shyamsunder, E., & Weissman, M. B. (1984) *Proc. Natl. Acad. Sci. U.S.A. 81*, 2359–2363.

Scheidt, W. R., & Gutermann, M. (1983) in *Iron Porphyrins* (Lever, A. B. P., & Gray, H. B., Eds.) Part I, pp 89–139, Table 4, p 109, Addison-Wesley, Reading, MA.

Scheidt, W. R., Haller, K. J., Fons, M., Mashiko, T., & Reed, C. A. (1981) *Biochemistry 20*, 3653–3657.

Sharonov, Y. A., Sharonova, N. A., Figlovsky, V. A., & Grigorjev, V. A. (1982) *Biochim. Biophys. Acta 709*, 332–341.

Spartalian, K., Lang, G., & Yonetani, T. (1976) *Biochim. Biophys. Acta 428*, 281–290.

Steigemann, W., & Weber, E. (1979) *J. Mol. Biol. 127*, 309–338.

Takano, T. (1977a) *J. Mol. Biol. 110*, 569–584.

Takano, T. (1977b) *J. Mol. Biol. 110*, 585–601.

Vincent, J. C., Kumar, C., & Chance, B. (1982) *Anal. Biochem. 126*, 86–93.

Waleh, A., & Loew, G. H. (1982) *J. Am. Chem. Soc. 104*, 2346–2351.

Woolery, G. L., Powers, L., Winkler, M., Solomon, E. I., & Spiro, T. G. (1984) *J. Am. Chem. Soc. 106*, 86–92.

Yen, L. (1971) Ph.D. Dissertation, The Ohio State University, Columbus, OH.